

## A modified discrete element model for sea ice dynamics

LI Baohui<sup>1,2,3,4,5</sup>, LI Hai<sup>4,5</sup>, LIU Yu<sup>4,5</sup>, WANG Anliang<sup>6</sup>, JI Shunying<sup>6\*</sup>

<sup>1</sup> Institute of Oceanology, Chinese Academy of Sciences, Qingdao 266071, China

<sup>2</sup> Key Laboratory of Ocean Circulation and Waves (KLOCAW), Chinese Academy of Sciences, Qingdao 266071, China

<sup>3</sup> Graduate School of Chinese Academy of Sciences, Beijing 100039, China

<sup>4</sup> National Marine Environment Forecast Center, State Oceanic Administration, Beijing 100081, China

<sup>5</sup> Key Laboratory of Research on Marine Hazards Forecasting, State Oceanic Administration, Beijing 100081, China

<sup>6</sup> State Key Laboratory of Structural Analysis for Industrial Equipment, Dalian University of Technology, Dalian 116023, China

Received 21 September 2010; accepted 11 March 2011

©The Chinese Society of Oceanography and Springer-Verlag Berlin Heidelberg 2014

### Abstract

Considering the discontinuous characteristics of sea ice on various scales, a modified discrete element model (DEM) for sea ice dynamics is developed based on the granular material rheology. In this modified DEM, a soft sea ice particle element is introduced as a self-adjustive particle size function. Each ice particle can be treated as an assembly of ice floes, with its concentration and thickness changing to variable sizes under the conservation of mass. In this model, the contact forces among ice particles are calculated using a viscous-elastic-plastic model, while the maximum shear forces are described with the Mohr-Coulomb friction law. With this modified DEM, the ice flow dynamics is simulated under the drags of wind and current in a channel of various widths. The thicknesses, concentrations and velocities of ice particles are obtained, and then reasonable dynamic process is analyzed. The sea ice dynamic process is also simulated in a vortex wind field. Taking the influence of thermodynamics into account, this modified DEM will be improved in the future work.

**Key words:** sea ice dynamics, modified discrete element model, contact force model, numerical simulation

**Citation:** Li Baohui, Li Hai, Liu Yu, Wang Anliang, Ji Shunying. 2014. A modified discrete element model for sea ice dynamics. *Acta Oceanologica Sinica*, 33(1): 56–63, doi: 10.1007/s13131-014-0428-3

### 1 Introduction

In the polar and sub-polar regions, sea ice plays an important role in the global climate and sometimes brings a series of engineering problems. To solve sea ice problems on various scales, the numerical simulations of sea ice dynamics have been investigated for decades. In the previous studies, most of the numerical models of sea ice dynamics were described with the continuum mechanics via the development of a series of numerical methods and constitutive model.

For the studies of numerical methods for sea ice dynamics, the Eulerian Finite Difference Method (FDM) (Hibler, 1979; Zhang and Lepparanta, 1995; Wu et al., 1998; Su et al., 2005), the Lagrangian smoothed particle hydrodynamics (SPH) and material-point method (Gutfraind and Savage, 1998; Ji et al., 2005; Sulsky et al., 2007), the coupled Lagrangian-Eulerian particle-in-cell (PIC) and Hybrid-Lagrangian-Eulerian (HLE) models (Flato, 1993; Liu et al., 2006; Ji et al., 2007) were developed. For the constitutive models, a viscous plastic (VP) model (Hibler, 1979), elastic plastic (EP) model (Coon et al., 1974), elastic-viscous-plastic model (Hunke and Dukowicz, 1997; Ji et al., 2005), and anisotropic models (Hibler, 2001; Coon et al., 1998; Pritchard, 1998) were established. With the numerical methods and constitutive models above, sea ice dynamics have been simulated numerically in various cold regions.

In the field observations and satellite images, it is shown that the sea ice clearly performs as granular materials, and a level ice, an ice ridge, a rafted ice and open water appear together (Tremblay and Mysak, 1997; Overland et al., 1998; Schulson, 2004). The ice floes have a wide size range, which can be more than 100 km on the large scale, or less than 1 m on the small scale (Overland et al., 1998; Dempsey, 2000; Hibler, 2001). This discrete distribution of sea ice has been noticed in the early 1980s, and it was observed that the ice cover performs as granular materials (Rothrock et al., 1984). The granular theory was adopted firstly to simulate the ice floe collision in broken ice fields with regular disks (Shen et al., 1986; Lepparanta et al., 1990). Recently, the ice particle has been modified as irregular, and has been applied in the formation of ice ridge on a meso-scale, and sea ice evolution in the arctic on a large scale (Hoyland, 2002; Hopkins et al., 2004; Hopkins and Thorndike, 2006).

In the DEM of sea ice dynamics, the ice field is divided into a series of discrete elements under Lagrangian coordinate. Each ice element has its own thickness, velocity and size. Considering the coagulation of ice floes, the ice breakup, rafting and ridging can also be simulated. The DEM has potentially good accuracy, as it has accurately fixed and free boundary edges to handle the complex boundary conditions. It can examine both aggregate and local behavior in an ice field. In addition, the

Foundation item: Special Fund of Marine Commonweal Industry under contact Nos 201105016 and 201205007, supported by National Marine Environment Forecasting Centre; the National Natural Science Foundation of China under contact No. 41176012.

\*Corresponding author, E-mail: jisys@dlut.edu.cn

DEM resembles the physical nature of sea ice dynamics. Therefore, the DEM of sea ice dynamics has the advantages of strong physical meaning, and high computational accuracy.

In the conventional DEM, the ice cover is described as rigid blocks with constant size and thickness, but the parameters of ice blocks cannot be determined accurately. Moreover, the high computational cost of DEM is its major shortcoming. Therefore, a modified DEM is introduced to sea ice dynamics in the present study. In this modified DEM, sea ice is modeled as an assembly of circular ice floes. Contacts are non-instantaneous and multiple contacts can occur simultaneously for each particle. Contact forces are modeled as viscous-elastic forces with a friction limit for the tangential component. Ridging effects are modeled by allowing particle size to change when contact stress exceeds a plastic yielding strength.

The novelty lies in the particle plastic deformation, which can model the ice rafting and ridging with dynamic particle size, thickness and concentration. To verify this modified DEM, two numerical cases of sea ice dynamics are carried out. One is the ice flow process in a channel with various widths, the other is the ice dynamics in a vortex wind field. Last, the improvements and applications of this model are discussed.

## 2 Modified discrete element model for sea ice dynamics

In this modified DEM, the ice particle is an assembly of ice floes. In this way, the contact force model of ice particles is related to its concentration and thickness. The ice particle size can be adjusted under the actions of external and internal ice forces. The normal contact force is determined by the plastic deformation of the ice particle. The ice rafting and ridging can be modeled by allowing the particle size and concentration to change when the normal contact stress exceeds its plastic yielding stress.

### 2.1 Momentum equation

The momentum equation for the motion of the ice element is governed by ice interactions, wind and water forces, Coriolis force, and ocean tilt effect. For each ice element, the momentum equation can be written as

$$M \frac{dV}{dt} = -MfK \times V + \tau_a + \tau_w - Mg\nabla\xi_w + F_c, \quad (1)$$

where  $M$  is the ice mass per unit area,  $M = N\rho_i h_i$ , where  $\rho_i$  is the ice density,  $h_i$  is the ice thickness, and  $N$  is the ice concentration;  $V$  is the ice velocity vector,  $f$  is the Coriolis parameter,  $K$  is the unit vector normal to the ice surface;  $\tau_a$  and  $\tau_w$  are the air and water stresses, here we have  $\tau_a = \rho_a C_a |V_{ai}| V_{ai}$ ,  $\tau_w = \rho_w C_w |V_{wi}| V_{wi}$ .  $\rho_a$  and  $\rho_w$  are the densities of air and current,  $C_a$  and  $C_w$  are the drag coefficients of wind and current.  $V_{ai}$  and  $V_{wi}$  are the wind and current velocity vectors relative to the ice;  $g$  is the gravity;  $\xi_w$  is the ice surface height, and  $F_c$  is the force vector of one ice particle contacting with its neighbors. The key to this momentum equation is to determine the contact force vector  $F_c$ .

### 2.2 Contact force model of sea ice particles

The discrete element model for granular material simulations was established in the late 1970s, and has been improved greatly recently. Here, we use a viscous-elastic model with the Mohr-Coulomb friction law to simulate interactions among ice particles.

The interactions among ice particles are determined with the elastic-viscous-plastic contact model. The contact force

model consists mainly of three components: normal and tangential damping forces proportional to velocity, normal and tangential elastic forces based on stiffness and overlap distance, and the shear sliding force based on the Mohr-Coulomb friction law. The contact force model is shown in Fig. 1, where  $M_A$  and  $M_B$  are the mass of ice particles A and B,  $K_n$  and  $K_s$  are the normal and tangential stiffness,  $C_n$  and  $C_s$  are the normal and tangential damping coefficients,  $\mu$  is the friction coefficient. Using the contact force model above, the normal and tangential forces of two contact particles can be calculated. While the two ice particles, the contact force vector  $F_c$  can be determined by considering the contact direction of the two particles.

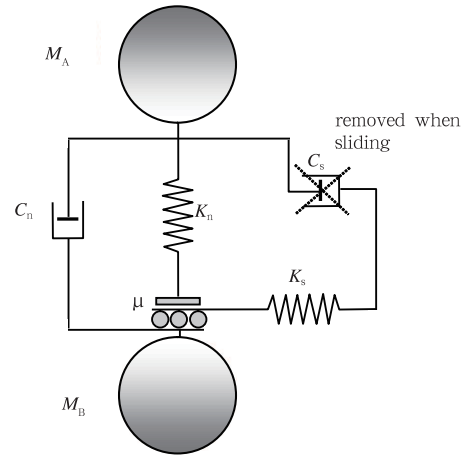


Fig.1. Contact force model for granular collision.

The normal force  $F_n$  consists of an elastic component  $F_e$  and a viscous component  $F_v$ , and also be determined with the plastic force when plastic deformation occurs of ice cover. While the normal force can be determined with

$$F_n = \min(F_e + F_v, F_p), \quad (2)$$

where the plastic force is calculated with

$$F_p = h_i N_i \tilde{D} \sigma_p, \quad (3)$$

where  $h_i$  and  $N_i$  are the ice thickness and concentration,  $\tilde{D}$  is the effective contact length of the two ice particles, and can be set as the mean diameters of the two ice particles.  $\sigma_p$  is the plastic force, and will be discussed in details in the next section.

The elastic and viscous forces can be written as

$$\begin{aligned} F_e &= K_n x_n, \\ F_v &= -C_n v_n, \end{aligned} \quad (4)$$

where  $x_n$  and  $v_n$  are the normal displacement and the normal velocity of two contact ice particles.

Consider the influence of ice concentration, the normal stiffness coefficient  $K_n$  can be written as a function of concentration as

$$K_n = E h_i \left( \frac{N_i}{N_{\max}} \right)^j, \quad (5)$$

where  $E$  is the elastic modulus;  $N_{\max}$  is the maximum ice concentration and  $j$  is an empirical constant. Usually, we have

$j=15$  (Shen et al., 1990).

The normal damping coefficient can be calculated as

$$C_n = \zeta_n \sqrt{2MK_n}, \quad (6)$$

$$\zeta_n = \frac{-\ln e}{\sqrt{\pi^2 + \ln^2 e}}, \quad (7)$$

where  $\zeta_n$  is the dimensionless normal damping coefficient,  $e$  is the restitution coefficient,  $M$  is the mean mass of two particles.

A slip condition is implemented on the tangential component. The tangential force is modeled by the spring-dashpot system until the friction limit, where the tangential force is then modeled by friction laws. The friction limit is defined as

$$F_t = \min(K_s x_s - C_s v_s, \mu F_n), \quad (8)$$

where  $v_s$  is the shear component of particle velocity; and  $\mu$  is the coefficient of friction. The normal and tangential stiffness and damping coefficients have the relationship of  $K_s = \alpha K_n$ ,  $C_s = \beta C_n$ . Usually, we have values of  $\alpha=1.0$ ,  $\beta=0.0$  (Ji et al., 2008).

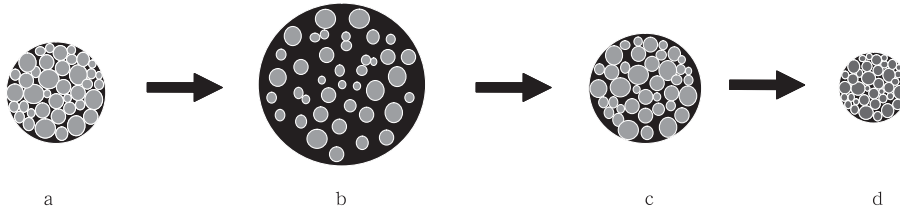


**Fig.2.** Dynamic evolution process of sea ice particle in the modified DEM.

The determination of the ice particle size, thickness and concentration are based on the calculation of the normal stress and the plastic deformation. The plastic deformation is modeled by changing the particle diameter, the concentration, and thickness, while the particle mass stays constant. The thickness only changes when concentration reaches a maximum limit. When rafting or ridging effects are induced, the normal elastic force is limited by a plastic stress  $\sigma_p$ . Ignoring the cohesion force among ice particles, the plastic stress was introduced by Shen et al. (1990) as

$$\sigma_p = \tan^2 \left( \frac{\pi}{4} + \frac{\phi}{2} \right) \left( 1 - \frac{\rho_i}{\rho_w} \right) \frac{\rho_i g h_i}{2} \left( \frac{N_i}{N_{\max}} \right)^j, \quad (9)$$

where  $\phi$  is the ice internal friction angle. If the normal stress exceeds  $\sigma_p$ , normal stress is set to  $\sigma_p$  and the plastic deformation occurs. In this way the model includes rafting and ridging effects. The plastic deformation is defined as the difference between the total deformation and the elastic deformation, where the total deformation is the compression distance  $x_n$ , and elastic deformation is deformation due to the maximum elastic stress,  $\sigma_p$ .

A Mohr-Coulomb yielding limit is imposed on the particles to represent ice ridging. Any stress exceeding the yielding criterion on the particle will result in particle deformation. The yielding criterion in the model is only dependent on the compressive stress and can be determined with Eq. (9). Considering the thermodynamics and adhesion among ice particles, the refreezing and break-up of the ice cover can be described accurately.

### 2.3 Normal contact force with plastic deformation

This modified DEM adopts the concept of smoothed particle of hydrodynamics (SPH) approach, and one ice particle is an assembly of small ice floes. Therefore, the ice particle is not a real ice block, with its statistical information depending on its ice floes inside.

In this modified DEM, the plastic deformation method is first proposed, which can describe the ice rafting and ridging. Since one particle in the DEM is constructed as an assembly of ice floes, the particle size can be adjusted based on the interactions with its neighbors, and its concentration and mean thickness can also be changed accordingly (Fig. 2). The sea ice floes have an initial dense packing in a sea ice package with high concentration (as shown in Fig. 2a). Under the wind and current actions, the ice cover can be packed into loose or dense conditions (as shown in Figs 2b–c). In the dynamic process of ice particle size, the total mass of the ice particle is constant. When the concentration approaches its maximum value  $N_{\max}$ , the mean thickness will increase with the decreasing of particle size (Fig. 2d).

### 2.4 Computational time step and ice particle neighbor searching

In the linear viscous-elastic contact force model, the binary contact time of two single particles can be defined as

$$T_{bc} = \frac{\pi}{\sqrt{\frac{2K_n}{M} (1 - \zeta_n^2)}}, \quad (10)$$

where  $T_{bc}$  is the binary contact time. In the linear force model, it is a constant determined by the particle size and material properties, and can be used to describe the granular flow characteristics. In the numerical simulation of the granular flow, the computational time step is usually set as 1/20 of the binary contact time.

In the DEM numerical simulation, particle contacts (particle overlaps) must be found to determine the resulting forces on the particles. Two search procedures exist which are typically used in determining particle overlap: grid search and direct search. In the Grid Search method, the domain of the ice floe is partitioned into a grid (Eulerian technology). The grid dimensions are determined such that only one particle can fit into a grid. When searching for particle contacts, only the neighboring cells of the particle of interest are investigated. The Direct Search method sets the frame of reference on the particle of interest (Lagrangian technology) as depicted. The distance between the centers of every pair of particle is calculated. If this distance is less than the sum of the diameters of the particles, they are stored as potential contacts. The grid system works well for floes of constant particle size. However, when dealing with variable size particles, it is not possible to make a grid sys-

tem where only one particle can fit into a grid. The present implementation of the modified DEM uses the direct search technique to detect particle-particle contacts.

### 3 Numerical Simulation of Sea Ice Dynamics with Modified DEM

To examine the reliability of this modified DEM, two numerical cases of sea ice dynamic processes in a channel with various widths and in a vortex wind field are simulated respectively.

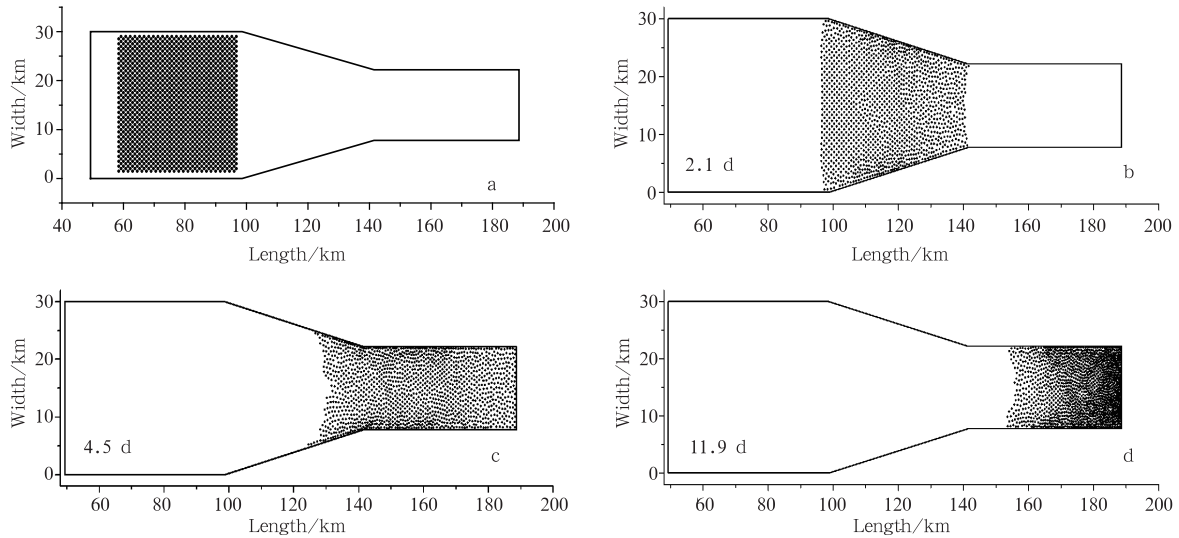


**Fig.3.** Distributions of ice particles in the channel simulated with the modified DEM.

**Table 1.** Parameters used in the ice ridging simulation

Parameter	Definition	Value	Parameter	Definition	Value
$B_l$	width of channel left side/km	30	$L$	initial ice length/km	190
$B_r$	width of channel right side/km	15	$D$	initial ice particle diameter/km	1.0
$t_{i0}$	initial ice thickness/m	0.2	$N_0$	initial ice concentration/%	80
$C_a$	wind drag coefficient	0.015	$V_a$	wind speed/m·s <sup>-1</sup>	10.0
$C_w$	current drag coefficient	0.004 5	$V_w$	current speed/m·s <sup>-1</sup>	0.2
$\rho_i$	ice density/kg·m <sup>-3</sup>	917	$\rho_w$	water density/kg·m <sup>-3</sup>	1 017
$\mu$	friction coefficient	0.5	$\phi$	friction angle of ice floe/(°)	46
$E$	young's Modulus/MPa	10	$\Delta t$	time step/s	1.83

With the modified DEM, the ice flow process in this channel with various widths is simulated, and the locations, velocity, concentration and thickness of ice particles are determined at various time steps. The simulated results are plotted in Figs 3–5. Under the given wind and current drags, the sea ice particles arrive at the end of the bell mouth of the channel after 2.1 d. After 4.5 d, the ice particles arrive at the end of the channel, then begin to raft and ridge under the drags of wind and current. After 11.9 d, the sea ice jams at the downstream boom and approaches a steady state. From the simulated results shown in Figs 3–5, we find that this modified DEM can successfully simulate the dynamics of ice flow. In the figures of ice velocity, we plot one velocity vector for 4 particles to clearly show the velocity distribution. In the simulation, the ice particle sizes are adjusted under the external forces induced with the wind and current drags, and the internal forces induced with the collisions between ice particles. Therefore, the concentrations and the thickness change with the deformation of ice particles. At the steady state shown in Fig. 5c, the ice concentration has the low values of 80% at the ice edge, and increases to the maximum val-

ues of 100% when approaching the channel end. The ice thickness also increases from the ice edge to the channel end. At the time of 4.5 d, the ice thickness at the boundaries of the channel when ice particles flow out the bell mouth is shown in Fig. 5e. At the steady state shown in Fig. 5f, the ice cover ridges at the end of the channel under the water and wind drag forces, and the maximum thickness is about 1.4 m.

### 3.1 Sea Ice Flow in a channel with various widths

A channel with various widths is covered by a uniform layer of ice with initial ice thickness  $t_{i0}$  and concentration  $N_{i0}$ . The layout of the channel is shown as Fig. 3a. Under the constant wind and current drags, the sea ice flows downstream, while the ice concentration and thickness change with the particle size. The input parameters are listed in Table 1.

At the time of 2.1 d, the ice particles have moved from the left side of the channel towards the right side, as shown in Fig. 3b. The ice concentration and thickness are higher in the narrower part of the channel.

At the time of 4.5 d, the ice particles have moved further downstream, as shown in Fig. 3c. The ice concentration and thickness are higher in the narrower part of the channel. At the time of 11.9 d, the ice particles have moved further downstream, as shown in Fig. 3d. The ice concentration and thickness are higher in the narrower part of the channel.

ues of 100% when approaching the channel end. The ice thickness also increases from the ice edge to the channel end. At the time of 4.5 d, the ice thickness at the boundaries of the channel when ice particles flow out the bell mouth is shown in Fig. 5e. At the steady state shown in Fig. 5f, the ice cover ridges at the end of the channel under the water and wind drag forces, and the maximum thickness is about 1.4 m.

### 3.2 Sea Ice Dynamics in a Vortex Wind Field

As a benchmark numerical case for sea ice dynamics, the ice drifting in a vortex wind field was constructed by Flato (1993) firstly to estimate the PIC method. Herein, this vortex wind field is also adopted to verify the modified DEM simulation. In this vortex wind field test, the upper half of the 500 km×500 km rectangular domain is covered by the uniform ice cover, with a thickness of 0.2 m and a concentration of 0.80, shown in Fig. 6. The lower half is open water. The vortex wind field is defined as (Flato, 1993)

$$W(r) = \min\left(\omega r, \frac{\lambda}{r}\right) k \times \frac{r}{r}, \quad (11)$$

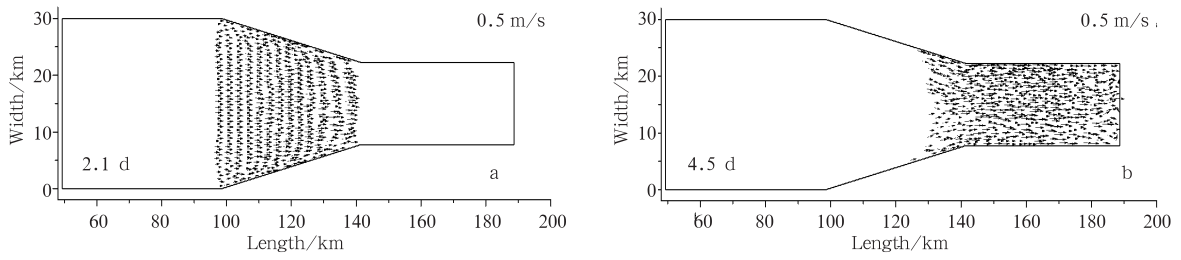


**Fig.4.** Ice thickness velocity distributions simulated with the modified DEM.

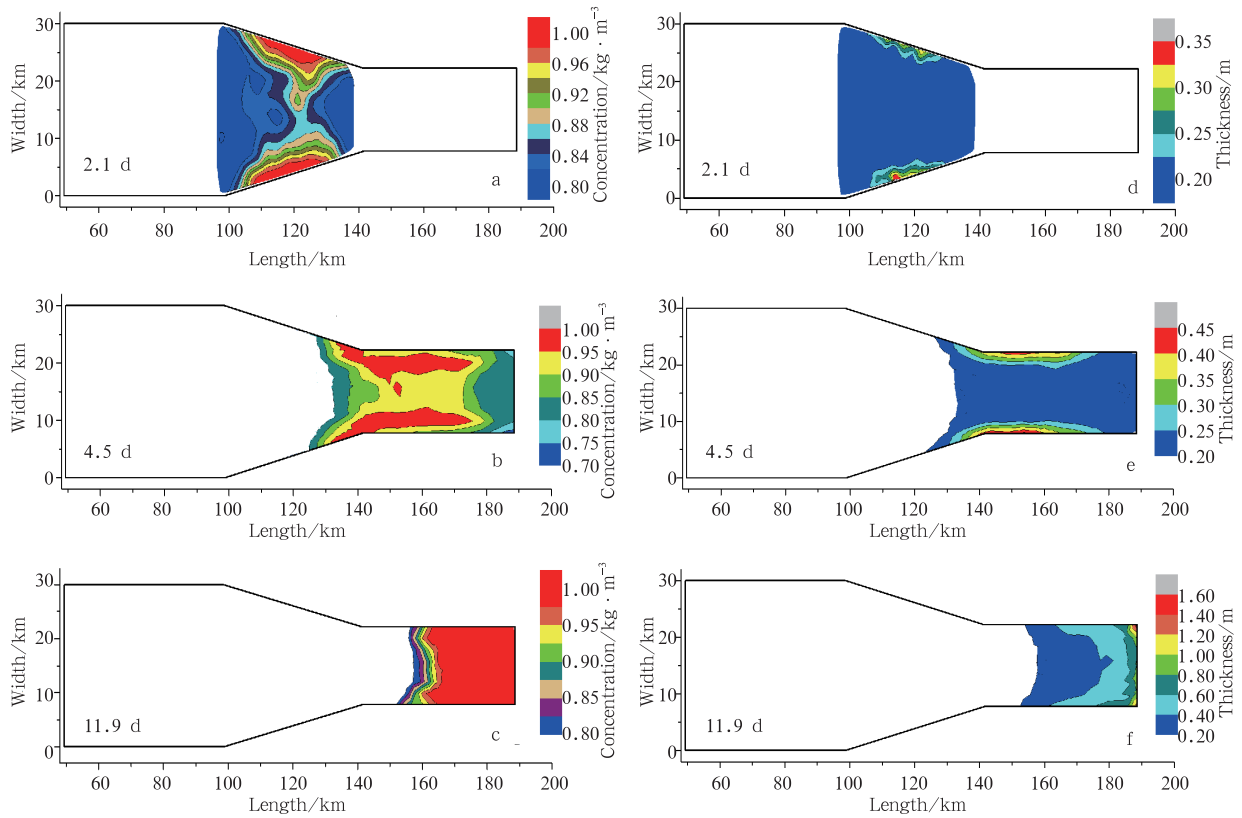


**Fig.5.** Ice concentration and thickness contours simulated with the modified DEM. Concentration (a, b, c) and Thickness (d, e, f)

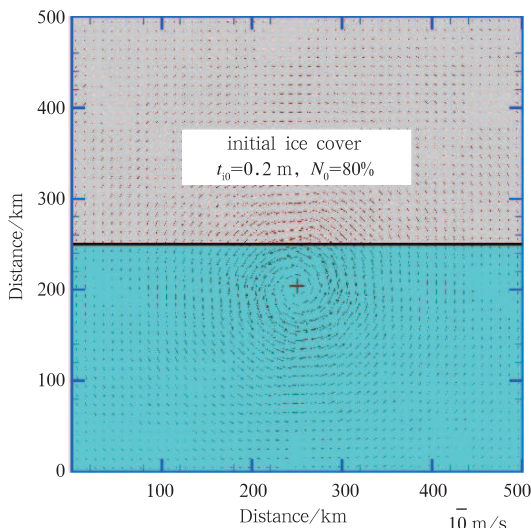


**Fig.6.** Vortex wind field and initial sea ice distribution.

where  $W$  is the wind vector,  $r$  is the distance to the vortex center,  $r$  is the position vector to the vortex center, and the vortex center position is (250 km, 200 km);  $\omega=0.5 \times 10^{-3} \text{ s}^{-1}$  and  $\lambda=8 \times 10^5 \text{ m}^2/\text{s}$ .

The sea ice dynamical process in this vortex wind field is simulated in 5 d with the modified DEM. The initial size of the ice particle is 5.0 km. Other input parameters are listed in Table 1. In this simulation, the time step is 6 s, the particle size is 5 km. The simulated ice particles locations, velocities and concentrations on the 1st, 3rd and 5th days are plotted in Figs 6–8. From the simulated particle locations shown Fig. 7, it can be found that the ice flows around the vortex center under the action of vortex wind. The simulated ice velocity, shown in Fig. 8a–c, has the similar distribution of the wind field, and is faster around the vortex wind center. For the ice concentration shown in Figs 8d–f, we can find that the ice concentration increases at the left boundary, and also has a convergent trend at the wind center. The ice edge around the vortex center has a sharp shape, which shows the high precision of this model.

**4 Conclusions**

The dynamics of ice cover perform as discontinuous materials on large and small scales in the polar and sub-polar oceans. To model the sea ice dynamics, a modified discrete element model (DEM) was developed. In this model, the sea ice particle is treated as an assembly of ice floes with variable conen-

tration and thickness. The interactions of ice particles is calculated with a viscous-elastic-plastic contact force model. In the dynamic process of ice drifting, the size of ice particle can be adjusted under the action of external and internal ice forces. The concentration and the thickness can also be determined accordingly based on the conservation of ice mass. The normal

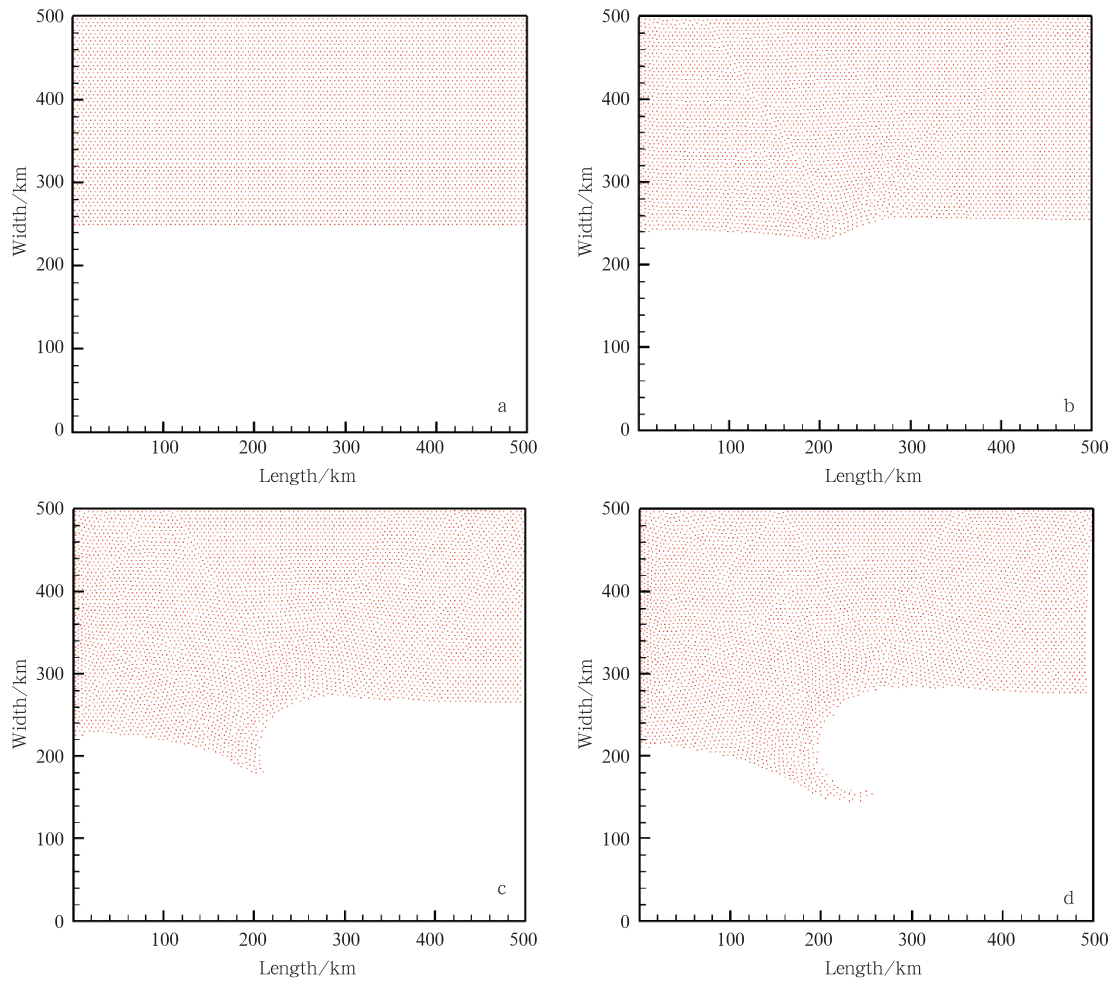


**Fig.7.** Sea ice particle location and ice concentration simulated with PIC model and modified DEM.

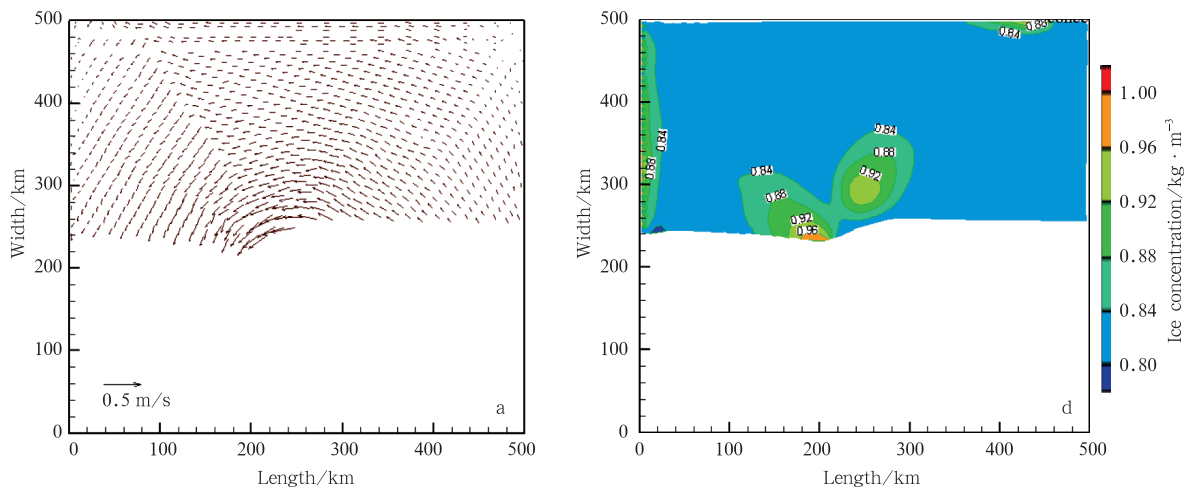


**Fig.8.**

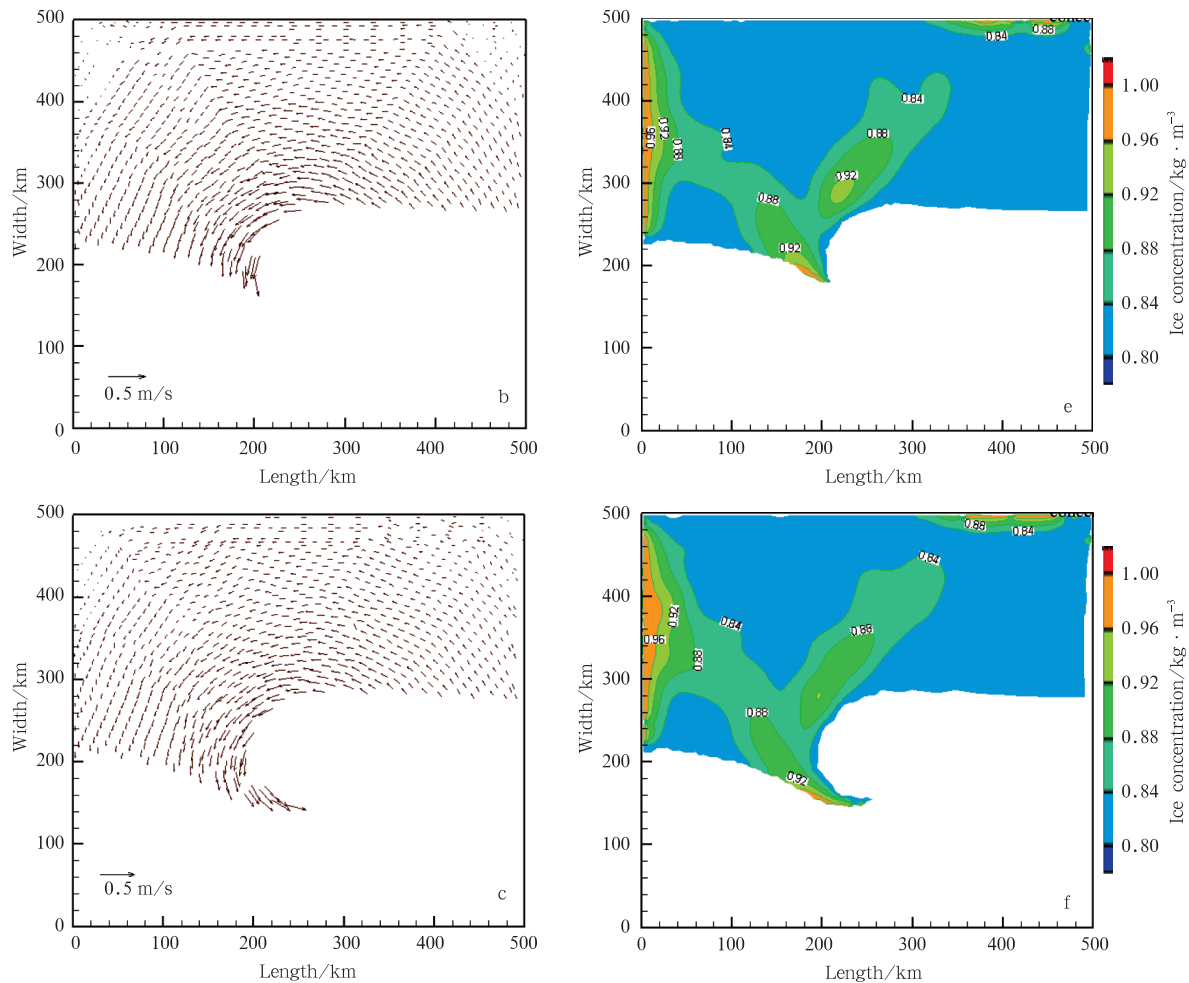


**Fig.8.** Velocity vector and concentration of sea ice simulated with modified DEM. Ice velocity (a, b and c) and ice concentration (d, e and f).

force between ice particles is limited with the plastic yielding, which can cause the rafting and ridging of ice cover. With this modified DEM, two numerical cases of the sea ice dynamics are carried out. One is the case of ice flow in a channel with various widths. The other is the case of ice drifting in a rectangular domain under a vortex wind field. Both of these cases showed the reasonable dynamic processes of the modified DEM.

In future studies, the thermodynamics and refreezing of ice floes will be considered to improve its accuracy. With this improvement, sea ice growth and drifting in natural oceans can be simulated with more reliability.

#### Acknowledgements

The authors would like to appreciate helpful discussions with Shen Hung Tao and Shen Hayley at Clarkson University, USA.

#### References

- Coon M D, Knoke G S, Echert D C, et al. 1998. The architecture of an anisotropic elastic-plastic sea ice mechanics constitutive law. *Journal of Geophysical Research*, 103(C10): 21915–21925
- Coon M D, Maykut S A, Pritchard R S, et al. 1974. modeling the pack ice as an elastic plastic material. *AIDJEX Bull*, 24: 1–105
- Dempsey J P. 2000. Research trends in ice mechanics. *International Journal of Solids and Structures*, 37: 131–153
- Flato G M. 1993. A Particle-in-cell Sea-ice Model. *Atmosphere and Oceanography*, 31(3): 339–358
- Gutfraind R, Savage S B. 1998. Flow of fractured ice through wedge-shaped channels: smoothed particle hydrodynamics and discrete-element simulations. *Mechanics of Materials*, 29: 1–17
- Hibler W D. 1979. A dynamic thermodynamic sea ice model. *Journal of Geophysical Oceanography*, 9: 817–846
- Hibler W D. 2001. Sea ice fracturing on the large scale. *Engineering Fracture Mechanics*, 68: 2013–2043
- Hopkins M A, Frankenstein S, Thorndike A S. 2004. Formation of an aggregate scale in Arctic sea ice. *Journal of Geophysical Research*, 109(C01032): 1–10
- Hopkins M A, Thorndike A S. 2006. Floe formation in Arctic sea ice. *Journal of Geophysical Research*, 111, C11S23, doi:10.1029/2005JC003352
- Hoyland K V. 2002. Simulation of the consolidation process in first-year sea ice ridges. *Cold Regions Science and Technology*, 34: 143–158
- Hunke E C, Dukowicz J K. 1997. An elastic-viscous-plastic model for sea ice dynamics. *Journal of Physical Oceanography*, 27: 1849–1867
- Lepparanta M, Lensu M, Lu Q M. 1990. Shear flow of sea ice in the Marginal Ice Zone with collision rheology. *Geophysica*, 25(1–2): 57–74
- Ji Shunying, Li Hai, Shen Hungtao, et al. 2007. A hybrid Lagrangian-Eulerian numerical model for sea ice dynamics. *Acta Oceanologica Sinica*, 26(5): 12–24

- Ji Shunying, Shen Hungtao, Wang Zhilian, et al. 2005. A viscoelastic-plastic constitutive model with Mohr-Coulomb yielding criterion for sea ice dynamics. *Acta Oceanologica Sinica*, 24(4): 54–65
- Ji Shunying, Wang Anliang, Li Hai, et al. 2008. Mechanical and numerical models for sea ice dynamics on small-meso scale. *Chinese Journal of Polar Science*, 19(2): 237–248
- Liu Yu, Wu Huiding, Zhang Zhanhai, et al. 2006. Modeling for the dynamic process of ice thickness variation using a particle-in-cell ice model. *Acta Oceanologica Sinica*, 28(2): 14–21
- Overland J E, McNutt S L, Salo S, et al. 1998. Arctic sea ice as a granular plastic. *Journal of Geophysical Research*, 103(C10): 21845–21868
- Pritchard R S. 1998. Ice conditions in an anisotropic sea ice dynamics model. *International Journal of Offshore and Ploar Engineering*, 8: 9–15
- Rothrock D, Thomdike A S. 1984. Measuring the sea ice grain size distribution. *Journal of Geophysical Research*, 89(C4): 6477–6486
- Schulson E M. 2004. Compressive shear faults within arctic sea ice: fracture on scales large and small. *Journal of Geophysical Research*, 109(C07016): 1–23
- Shen H H, Hibler W D, Lepparanta M. 1986. On applying granular flow theory to a deforming broken ice field. *Acta Mechanica*, 63: 143–160
- Shen H T, Shen H H, Tsai S M. 1990. Dynamic transport of river ice. *Journal of Hydraulic Research*, 28(6): 659–671
- Su Jie, Wu Huiding, Bai Shan, et al. 2005. A coupled ice-ocean model for the Bohai Sea: II. Case study. *Acta Oceanologica Sinica*, 24(3): 54–67
- Sulsky D, Schreyer H, Peterson K, et al. 2007. Using the material-point method to model sea ice dynamics. *Journal of Geophysical Research*, 112: C02S90, doi: 10.1029/2005JC003329
- Tremblay L B, Mysak L A. 1997. Modeling sea ice as a granular material, including the dilatancy effect. *Journal of Physical Oceanography*, 27: 2342–2360
- Wu Huiding, Bai Shan, Zhang Zhanhai. 1998. Numerical simulation for dynamical processes of sea ice. *Acta Oceanologica Sinica*, 16(3): 303–325
- Zhang Z H, Lepparanta M. 1995. Modeling the influence of ice on sea level variations in the Baltic Sea. *Geophysical Research*, 31(2): 31–45